Solvent-Modulated Ground-State Rotamerism and Tautomerism and Excited-State Proton-Transfer Processes in *o*-Hydroxynaphthylbenzimidazoles

Alfonso Brenlla, Flor Rodríguez-Prieto,* Manuel Mosquera, Miguel A. Ríos, and M. Carmen Ríos Rodríguez*

Departamento de Química Física, Facultade de Química, Universidade de Santiago de Compostela, E-15782 Santiago de Compostela, Spain

Received: August 26, 2008; Revised Manuscript Received: November 4, 2008

The ground-state rotamerism and tautomerism and the excited-state proton-transfer processes of 2-(1′-hydroxy-2′-naphthyl)benzimidazole (**1**) and 2-(3′-hydroxy-2′-naphthyl)benzimidazole (**2**) have been investigated in various solvents by means of UV−vis absorption spectroscopy, steady-state and time-resolved fluorescence spectroscopy, and quantum-mechanical ab initio calculations. For both compounds, a solvent-modulated rotameric equilibrium, and also tautomeric for **1**, was observed in the ground state. In apolar solvents, both **1** and **2** exist as planar syn normal forms, with the hydroxyl group hydrogen bonded to the benzimidazole N3. In acetonitrile and ethanol, a rotameric equilibrium is established between the syn form and its planar anti rotamer, with the phenyl ring rotated 180° about the C2−C2′ bond. In ethylene glycol, glycerol, and aqueous solution with 40% ethanol, a tautomeric equilibrium was detected for **1** between the syn and anti normal forms and the tautomer form, with the hydroxyl proton transferred to the benzimidazole N3. In all of the solvents studied, the syn normal form of **1** and **2** undergoes an ultrafast excited-state intramolecular proton transfer (ESIPT) to yield the excited tautomer. The anti normal forms of **1** and **2**, unable to experience ESIPT, give normal form fluorescence. In addition, the anti normal conformer of **2** partly deprotonates at the hydroxyl group in aqueous solution with 40% ethanol, giving the excited anion. The monocations of **1** and **2**, protonated at the benzimidazole N3, are strong photoacids that deprotonate completely in aqueous solution with 40% ethanol and to a great extent in ethanol, giving the excited tautomer.

Introduction

Proton transfer is an elementary reaction that plays a crucial role in processes so relevant for life as DNA mutation and repair,[1] photosynthesis,[2] and respiration.[3] Because of its involvement in many chemical and biological processes, proton transfer has been the focus of considerable experimental and theoretical work;[4] however, in spite of the progress in the field, the detailed mechanism of proton transfer is still not fully understood.

A special class of proton-transfer reactions is that constituted by those proton-transfer processes taking place in the excited state. Molecules possessing acid and/or basic groups are known to experience an enhancement of acidity and/or basicity (changes of 7 units or more in the pK_a value are common) of those groups upon excitation. Specifically, molecules having an acid group (typically a hydroxyl group) and a basic site (generally oxygen or nitrogen) hydrogen bonded in the ground state may undergo an ultrafast excited-state intramolecular proton transfer, ESIPT, from the acid to the basic site.[5,6] ESIPT molecules have applications as laser dyes,[7,8] UV photostabilizers,[9] membrane and protein probes,[10,11] and are potential components for photoswitches[12,13] and organic LEDs.[14,15]

Molecules with an increased acidity in the excited state (photoacids) may experience a deprotonation upon excitation in the presence of basic species (typically the solvent). Photoacids have important applications as polymerization initiators,[16] in molecular machines,[17] or as a way of creating a rapid pH change (pH jump).[18] Also, the fact that the acid is instantaneously generated by light absorption ($\sim 10^{-15}$ s), together with the nowadays availability of ultrafast spectroscopic techniques, makes photoacids very interesting probes to investigate the detailed mechanism of proton-transfer processes.[19] In this sense, we have recently reported[20] that the strong photoacid cations 6-hydroxyquinolinium and 6-hydroxy-1-methylquinolinium undergo in the first excited singlet state an ultrafast proton transfer to water and alcohols, the reaction rate being controlled by solvation. It would be very interesting to investigate other photoacids showing an efficient excited-state deprotonation in alcohols but for which the intrinsic proton transfer is not so rapid as that observed in the compounds above.

2-(2′-hydroxyphenyl)benzimidazole, HBI,[5,6,21−28] 2-(4′-amino-2′-hydroxyphenyl)benzimidazole, AHBI,[29] 2-(4′-*N*,*N*-diethylamino-2′-hydroxyphenyl)benzimidazole, DEHBI,[29] and 2-(3′-hydroxy-2′-pyridil)benzimidazole, HPyBI,[30] (Chart 1) are examples of ESIPT molecules studied in our group. A solvent-modulated ground-state rotameric and tautomeric equilibrium was observed for these benzimidazole derivatives. In apolar aprotic solvents, these compounds exist in the ground state as the planar syn normal form $\mathbf{N_{syn}}$ (Chart 1), with an intramolecular hydrogen bond N···H−O, this species undergoing in the excited state an intramolecular proton transfer from the hydroxyl group to the benzimidazole N3 to yield tautomer **T***. In protic solvents, a ground-state rotameric equilibrium between $\mathbf{N_{syn}}$ and its planar anti rotamer $\mathbf{N_{anti}}$ (Chart 1) was detected for HBI, AHBI, and DEHBI. $\mathbf{N_{anti}}$, unable to undergo ESIPT, yields normal $\mathbf{N^*_{anti}}$ emission upon excitation. In spite of the similar structures of these hydroxyphenylbenzimidazoles, in aqueous solution an equilibrium between $\mathbf{N_{syn}}$, $\mathbf{N_{anti}}$, and **T** is established in the ground state for HBI, whereas only $\mathbf{N_{anti}}$ and **T** were

* To whom correspondence should be addressed. E-mail: carmen.rios@usc.es (M.C.R.R.), flor.rodriguez.prieto@usc.es (F.R.-P.).

10.1021/jp8076003 CCC: $40.75
Published on Web 12/15/2008

CHART 1: Molecular Structures of HPyBI, HBI, AHBI, and DEHBI. The Neutral Forms (N_{syn}, N_{anti}, and T) and the Monocation (C) Are Shown

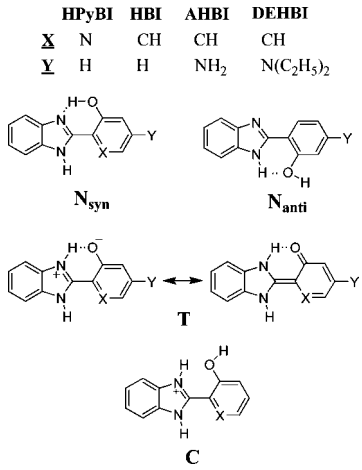

detected for its derivatives AHBI and DEHBI and only $\mathbf{N}_{syn}$ and **T** for HPyBI. For all of these compounds, $\mathbf{N}^*_{syn}$ experienced an ESIPT process in aqueous solution to give **T***. However, whereas for HBI a fraction of $\mathbf{N}^*_{anti}$ molecules dissociate to give the anion in aqueous solution, for the derivatives AHBI and DEHBI this process was not observed. These results reveal that protic solvents play a crucial role in stabilizing species other than $\mathbf{N}_{syn}$, and therefore in these solvents excited-state processes different than ESIPT can be observed. It is also clear that a small modification in HBI structure may induce a different ground- and excited-state behavior of the compound.

We also found that the monocation **C** of HBI[27] and HPyBI,[31] protonated at the benzimidazole N3 (Chart 1), is a strong photoacid, which deprotonates completely in aqueous solution and to a great extent in ethanol. In acetonitrile, we proved that the excited monocation of HBI[32] is able to deprotonate if low concentrations of weak bases (water, dimethyl sulfoxide, and urea) are added.

In this work we investigate the ground-state rotamerism and tautomerism and the excited-state proton-transfer processes, in various solvents, of the HBI analogues 2-(1′-hydroxy-2′-naphthyl)benzimidazole, **1**, and 2-(3′-hydroxy-2′-naphthyl)benzimidazole, **2** (Chart 2). The monocations of the naphthol derivatives **1** and **2** are, in view of their structural similarity with the monocation of HBI, potential strong photoacids. Most of the investigations on the dissociation mechanism of photoacids refer to neutral or anionic species. The dissociation mechanism of cationic photoacids (like those of **1** and **2**) can be different, as the efficiency of the geminate recombination of the conjugate base and the proton must be dependent on the charge of the conjugate base. Furthermore, **1** and **2** may also undergo ESIPT. In fact, ESIPT has been reported for **2** in acetonitrile and alcohols by Douhal et al.[33] A ground-state rotameric equilibrium was reported in these solvents between a planar normal form with an intramolecular hydrogen bond N···H−O (Chart 2), undergoing ESIPT upon excitation to give the tautomer, and a rotamer without this intramolecular hydrogen bond, yielding in the excited state the normal form fluorescence. However, the behavior of **2** in aqueous solution or in other solvents in non-neutral conditions was not reported. To our knowledge, no studies on the photophysics of **1** have been published.

The main objectives of this work are to investigate (1) the influence of the relative position of the hydroxyl group on the ground-state rotamerism and tautomerism of **1** and **2** in various solvents and on the photoinduced proton-transfer processes undergone by the species involved in these equilibria, and (2) the excited-state deprotonation of the monocations of **1** and **2** in various solvents, to test the adequacy of these monocations to be employed later as photoacids in mechanistic studies.

CHART 2: Molecular Structures of 1 and 2 Studied in This Work[a]

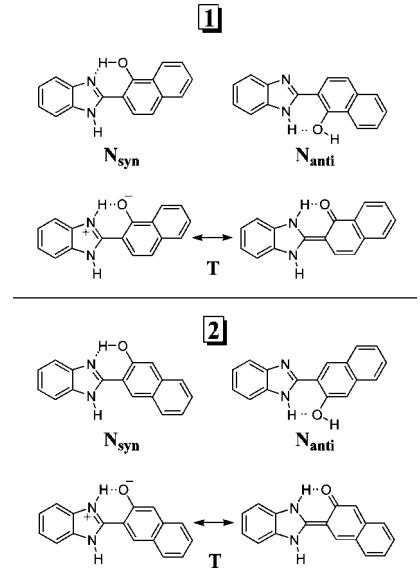

[a] The normal forms ($\mathbf{N}_{syn}$ and $\mathbf{N}_{anti}$) and the tautomer (**T**) are shown.

Experimental Section

Materials. **1** and **2** were prepared by condensation of 1,2-benzenediamine (15.9 mmol, Aldrich) with 1-hydroxy-2-naphthoic acid (14.9 mmol, Aldrich) or 2-hydroxy-3-naphthoic acid (14.9 mmol, Aldrich), respectively, in polyphosphoric acid (Merck) at 170−190 °C as described for other benzimidazole derivatives.[34] The final products were recrystalized from ethanol−water several times, and their purity was checked by fluorescence and their structure confirmed by ^{1}H. Compound **1**.^{1}H NMR (300 MHz, dimethyl sulfoxide-d_6), δ (ppm): 7.30 (b, 2H), 7.54 (d, 1H, J = 8.8 Hz), 7.60 (m, 2H), 7.73 (b, 2H), 7.90 (d, 1H, J = 7.9 Hz), 8.08 (d, 1H, J = 8.7 Hz), 8.83 (dd, 1H, J = 0.9 Hz, J = 8.0 Hz). Compound **2**. ^{1}H NMR (300 MHz, dimethyl sulfoxide-d_6), δ (ppm): 7.31 (b, 2H), 7.37 (td, 1H, J = 1.0 Hz, J = 7.5 Hz), 7.41 (s, 1H), 7.49 (td, 1H, J = 1.0 Hz, J = 7.0 Hz), 7.70 (b, 2H), 7.78 (d, 1H, J = 8.1 Hz), 7.88 (d, 1H, J = 8.1 Hz), 8.70 (s, 1H).

Methods. Solutions were made up in double-distilled water and in spectroscopy-grade solvents and were not degassed. Aqueous solutions always contained 40% (v/v) ethanol, due to the low solubility of the compounds in pure water. Acidity was varied with $HClO_4$ in acetonitrile and ethanol and with $HClO_4$, or acetic acid/sodium acetate or ammonium perchlorate/ammonia buffers in aqueous solutions. In all of the solvents, pH_c was calculated as $-\log([H^+]/\text{mol dm}^{-3})$. All experiments were carried out at 25 °C.

UV−vis absorption spectra were recorded in a Varian Cary 3E spectrophotometer. Fluorescence excitation and emission spectra were recorded in a Jovin Yvon - Spex Fluoromax-2 spectrofluorometer, with correction for instrumental factors by means of a reference photodiode and correction files supplied by the manufacturer. Fluorescence quantum yields were measured using quinine sulfate ($<3 \times 10^{-5}$ mol dm^{-3}) in aqueous

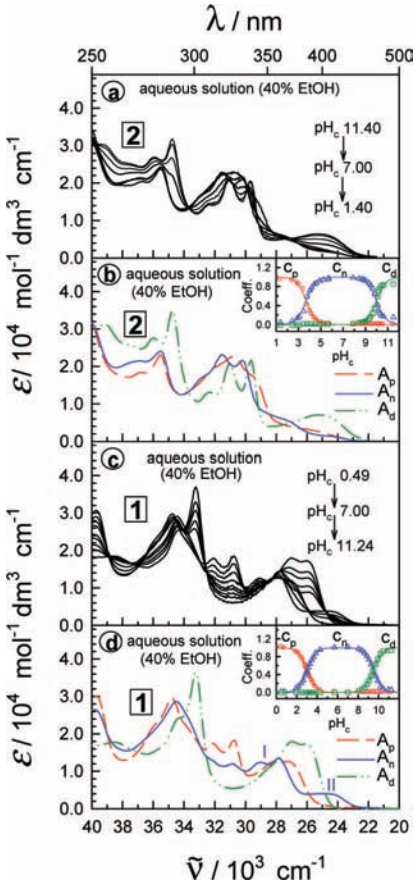

Figure 1. (a) Absorption spectra of **2** in aqueous solution (with 40% ethanol) at various pH_c values between 1.40 and 11.40. (b) Absorption spectra of the neutral, protonated, and deprotonated forms of **2** and their experimental (symbols) and calculated (solid lines) acidity-dependent contributions (inset) obtained applying PCGA to the series of absorption spectra in part (a). (c) Absorption spectra of **1** in aqueous solution (with 40% ethanol) at various pH_c values between 0.49 and 11.24. (d) Absorption spectra of the neutral, protonated, and deprotonated forms of **1** and their experimental (symbols) and calculated (solid lines) acidity-dependent contributions (inset) obtained applying PCGA to the series of absorption spectra in part (c).

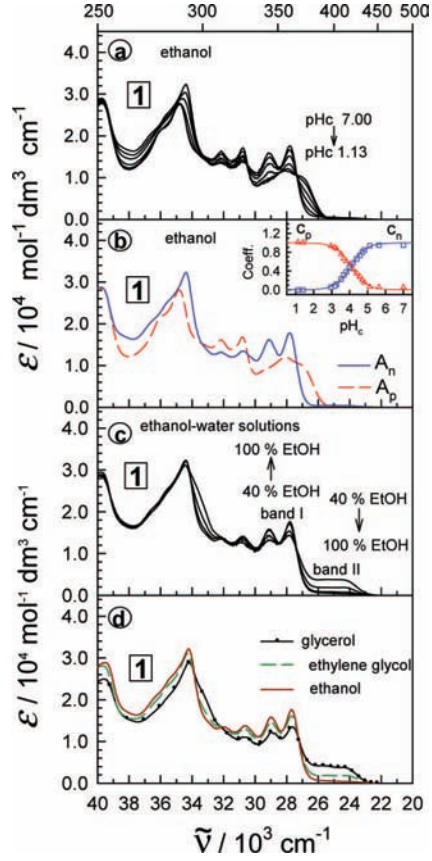

Figure 2. (a) Absorption spectra of **1** in ethanol at various pH_c values between 1.13 and 7.00. (b) Absorption spectra of the neutral and protonated forms of **1** and their experimental (symbols) and calculated (solid lines) acidity-dependent contributions (inset) obtained applying PCGA to the series of absorption spectra in part (a). (c) Absorption spectra of **1** in ethanol−water mixtures between 40 and 100% ethanol (v/v). (d) Absorption spectra of **1** in ethanol, ethylene glycol, and glycerol.

H_2SO_4 (0.5 mol dm^{-3}) as standard ($\phi = 0.546$).[35,36] Fluorescence lifetimes were determined by single-photon timing in an Edinburgh Instruments FL-900 spectrometer equipped with a hydrogen-filled nanosecond flash lamp and in an Edinburgh Instruments LifeSpec-ps spectrometer provided with a 375 nm diode laser. The reconvolution analysis software supplied by the manufacturer was employed.

Theoretical equations were fitted to the experimental data by means of a nonlinear weighted least-squares routine based on the Marquardt algorithm. Principal component global analyses were performed with *Matlab 6.5* for Windows.

Quantum-mechanical ab initio calculations were performed using the *Gaussian '03* software package.[37]

Results

1. Absorption Spectra and Acid−Base Equilibria in the Ground State. Some absorption spectra recorded for **2** in aqueous solutions with 40% ethanol between pH_c 1.40 and 11.40 are shown in part a of Figure 1. The absorption spectrum obtained under neutral conditions peaked at 31 550 cm^{-1} and showed a shoulder at about 28 000 cm^{-1}. Upon decreasing the pH_c, the absorption spectrum shifted slightly to the red, and a new spectrum, with maximum at 30 670 cm^{-1} and a weak band at ~27 000 cm^{-1}, was recorded at $pH_c < 2$. On going from neutral to basic conditions, the absorption spectrum shifted to the red, with a new spectrum, peaking at 29 630 cm^{-1} and showing a weaker band at 25 250 cm^{-1}, being detected at $pH_c > 11$.

The absorption spectra of **1** in aqueous solution with 40% ethanol were measured between pH_c 0.49 and 11.24 (some of the spectra are plotted in part c of Figure 1). The spectrum obtained under neutral conditions showed a structured and intense band (band I) at 27 860 cm^{-1}, accompanied by a weak band at ~25 000 cm^{-1} (band II). Absorption band I shifted to the red as the pH_c decreased, a new spectrum peaking at 27 250 cm^{-1} being obtained at $pH_c < 1$. Upon increasing the pH_c from neutral conditions, band I shifted to the red, with a spectrum showing a structured first absorption band with maximum at 26 950 cm^{-1} being detected at $pH_c > 11$.

The absorption spectrum of **1** in neutral ethanol (part a of Figure 2) showed a structured first absorption band located at about the same position as that of absorption band I detected in water but with a higher molar absorption coefficient (1.8×10^4 mol^{-1} dm^3 cm^{-1} in ethanol and 1.3×10^4 mol^{-1} dm^3 cm^{-1} in water). Absorption band II was however absent in this solvent. Upon acidification of the alcohol, the first absorption band shifted to the red and the molar absorption coefficient decreased, with a new spectrum being obtained at pH_c ~1.

The absorption spectra of **1** in ethanol−water mixtures in the range 40−100% ethanol are shown in part c of Figure 2. It

TABLE 1: Relative Energies *E* and Dipole Moments μ for Various Conformers and Tautomers of 1 in the Ground State, Obtained by Quantum Mechanical ab Initio Calculations at the B3LYP/6-31G Level in the Gas Phase and in Water (with PCM Continuum Model)**

	Gas Phase		Water	
form	*E*/kJ mol^{-1}	μ/D	*E*/kJ mol^{-1}	μ/D
$\mathbf{N}_{syn}$	0	3.23	0	5.43
$\mathbf{N}_{anti}$	38.1	4.61	28.4	7.39
T	18.0	5.04	6.9	8.48

is seen that the intensity of band I increased with the ethanol content, whereas that of band II decreased, this band being hardly detected in pure ethanol, and several isosbestic points were detected. The absorption spectra were also measured in glycerol and ethylene glycol and compared with that measured in ethanol (part d of Figure 2). The contribution of band II to the absorption spectrum increased in the series ethanol < ethylene glycol < glycerol, whereas that of band I showed the reverse trend and various isosbestic points were detected.

2. Quantum-Mechanical ab Initio Calculations. B3LYP ab initio calculations were performed for the ground-state syn normal form $\mathbf{N}_{syn}$, its anti rotamer $\mathbf{N}_{anti}$, and the tautomer **T** of **1** (Chart 2), at the 6-31G** level both in the gas phase and in water employing the polarized continuum model (PCM). The energies and dipole moments obtained are compiled in Table 1.

3. Fluorescence Spectra and Lifetimes. ***Neutral Media.*** The fluorescence spectra of **1** in cyclohexane (part a of Figure 3) were structured and independent of the excitation wavenumber.

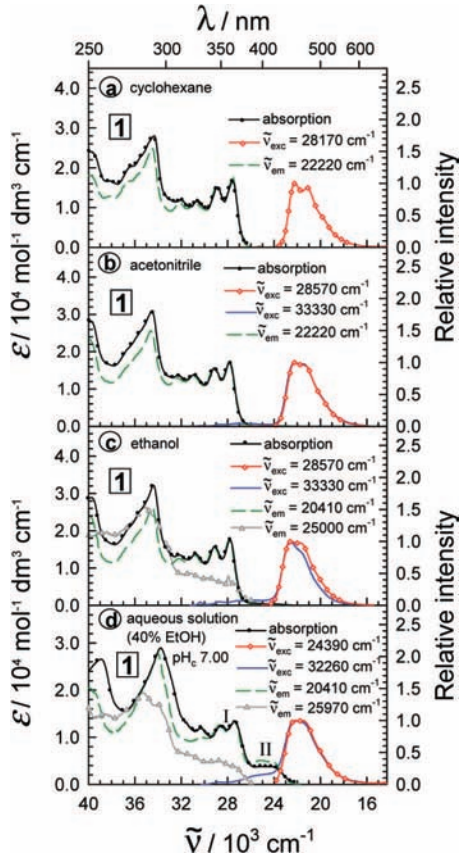

Figure 3. Normalized fluorescence excitation and emission spectra of **1** in (a) cyclohexane, (b) acetonitrile, (c) ethanol, and (d) aqueous solution (with 40% ethanol) of pH_c 7.00, together with the absorption spectra in the same solvents.

TABLE 2: Fluorescence Quantum Yields of 1 and 2 in Various Solvents and Acidity Conditions at 298 K; Shown in Brackets Are the Species to Which the Emission Was Assigned

solvent	ϕ (**1**)	ϕ (**2**)
	neutral media	
cyclohexane	0.274 [**T***]	
acetonitrile	0.255 [**T***]	0.043 [$\mathbf{N}^*_{anti}$ and **T***]
ethanol	0.327 [**T***]	0.088 [$\mathbf{N}^*_{anti}$ and **T***]
aqueous solution (40% EtOH)	0.230 [$\mathbf{N}^*_{anti}$ and **T***] (band I excitation) 0.145 [**T***] (band II excitation)	0.100 [$\mathbf{N}^*_{anti}$, **A***, and **T***]
	acid media	
acetonitrile	0.371 [**C***]	0.226 [**C***]
ethanol	0.332 [**C*** and **T***]	0.076 [**C*** and **T***]
aqueous solution (40% EtOH)	0.168 [**T***]	0.057 [**T***]
	basic media	
aqueous solution (40% EtOH)	~0[a]	0.229 [**A***]

[a] No fluorescence was detected for **1** in basic solution.

The emission band showed an exceptionally large Stokes shift and a fluorescence quantum yield of 0.274 (Table 2). The excitation and absorption spectra were almost coincident in the first absorption band region. Furthermore, the fluorescence decay was monoexponential (Table 3) with a decay time of 1.69 ns.

The fluorescence spectra of **1** in acetonitrile and ethanol (parts b and c of Figure 3) were qualitatively similar to that reported in cyclohexane, except for the fact that in both acetonitrile and ethanol the main fluorescence band (peaking at ~22 000 cm^{-1}) obtained under excitation at 33 300 cm^{-1} was accompanied by a weak emission at about 26 000 cm^{-1}. In both solvents, the excitation spectrum measured at the maximum of the emission band almost coincided with the absorption spectrum, and the fluorescence quantum yields were similar to that measured in cyclohexane (Table 2). The excitation spectrum measured in ethanol at 25 000 cm^{-1} was located at about the same position as the spectrum recorded at the maximum of the emission band. The fluorescence decay could only be monitored at the main emission band. A monoexponential decay was obtained for both solvents with decay times of 1.44 and 1.65 ns in acetonitrile and ethanol, respectively (Table 3).

The fluorescence spectra of **1** in aqueous solution with 40% ethanol were similar to those reported in pure ethanol (part d of Figure 3), except for the fact that the excitation spectrum obtained at $\tilde{\nu}_{em} = 20\,410$ cm^{-1} showed, besides the structured excitation band I detected in the other solvents, a weak band at about 25 000 cm^{-1} (band II). A single emission band peaking at ~22 100 cm^{-1}, which overlapped excitation band II, was obtained under excitation at band II. This emission band was also detected under excitation at band I, but, as previously observed in ethanol and acetonitrile, this fluorescence band was accompanied by a weak emission at about 25 000 cm^{-1}. Furthermore, the excitation spectrum recorded at $\tilde{\nu}_{em} = 20\,410$ cm^{-1} showed a higher contribution of band II than the absorption spectrum. The fluorescence quantum yields obtained under excitation at bands I and II were 0.230 and 0.145, respectively (Table 2). The fluorescence decay of **1** in aqueous solution of pH_c 7.00 with 40% ethanol under excitation at 28 570 cm^{-1} (band I) was monoexponential in the range 20 830−22 730 cm^{-1} with a decay time of 1.70 ns (Table 3). A biexponential fluorescence decay was however obtained, with a decay time of 1.77 ns (92%) and a second decay time of 4.7 ns (8%), when

TABLE 3: Fluorescence Decay Times τ and Associated Percentages (in Parentheses) of 1 in Various Solvents at 298 K; Shown in Brackets Are the Species to Which Each Decay Time Was Assigned

solvent	$\tilde{\nu}_{exc}$/cm^{-1}	$\tilde{\nu}_{em}$/cm^{-1}	τ_1/ns	τ_2/ns	χ^2
			neutral media		
cyclohexane	32 260	22 220	1.689 ± 0.007 [**T***]		1.037
acetonitrile	27 770	22 730	1.436 ± 0.003 [**T***]		1.175
	27 770	20 410	1.448 ± 0.003 [**T***]		1.074
ethanol	27 770	22 730	1.630 ± 0.003 [**T***]		1.157
	27 770	21 510	1.656 ± 0.003 [**T***]		1.193
	27 770	20 410	1.655 ± 0.003 [**T***]		1.154
aqueous solution	33 900	24 390	1.774 ± 0.014 (92%) [**T***]	4.7 ± 0.2 (8%) [$\mathbf{N^*_{anti}}$]	1.148
(pH_c 7.00, 40% EtOH)	28 570	20 830	1.708 ± 0.003 [**T***]		1.155
	28 570	21 740	1.698 ± 0.003 [**T***]		1.232
	28 570	22 730	1.701 ± 0.003 [**T***]		1.186
			acid media		
acetonitrile	27 770	26 320	2.300 ± 0.003 [**C***]		1.121
($[HClO_4] = 1.3 \times 10^{-3}$ mol dm^{-3})	27 770	24 390	2.299 ± 0.003 [**C***]		1.143
	27 770	22 470	2.302 ± 0.003 [**C***]		1.126
ethanol	30 030	25 640	1.666 ± 0.011 (35%) [**T***]	0.682 ± 0.004 (65%) [**C***]	1.109
(pH_c 1.26)	30 030	23 810	1.659 ± 0.005 (48%) [**T***]	0.435 ± 0.002 (53%) [**C***]	1.176
	30 030	21 740	1.746 ± 0.002 (—)[a] [**T***]	0.41 ± 0.02 (—)[a] [**C***]	1.041
aqueous solution	26 810	22 730	1.740 ± 0.001 [**T***]		1.112
(pH_c 1.50, 40% EtOH)	26 810	20 830	1.726 ± 0.003 (94%) [**T***]	6.1 ± 0.2 (6%)[b]	1.162

[a] The percentages cannot be calculated because the associated amplitude of the short lifetime is negative. [b] Decay time probably due to an impurity.

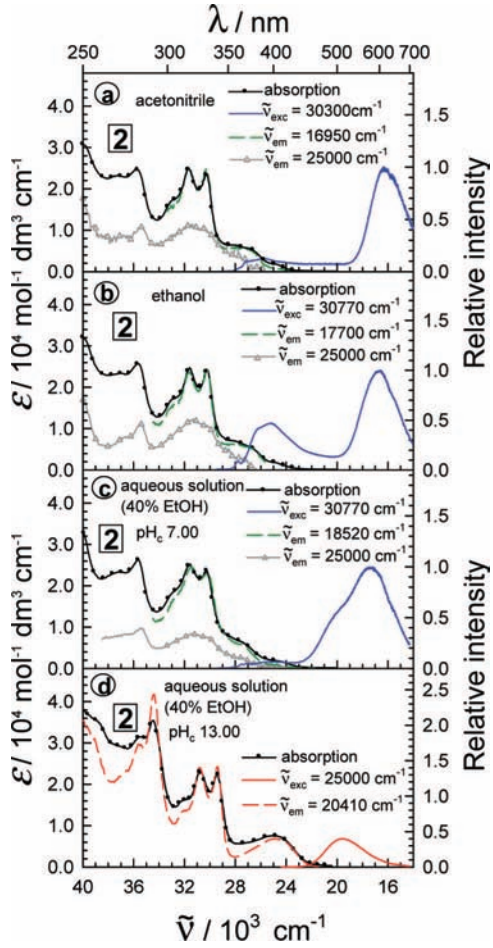

Figure 4. Normalized fluorescence excitation and emission spectra of **2** in (a) acetonitrile, (b) ethanol, (c) aqueous solution (with 40% ethanol) of pH_c 7.00, and (d) aqueous solution (with 40% ethanol) of pH_c 13.00, together with the absorption spectra in the same solvents.

monitored at the weak emission band (24 390 cm^{-1}) under excitation at 33 900 cm^{-1}.

The fluorescence spectra of **2** in acetonitrile and ethanol (parts a and b of Figure 4) were very similar. The emission spectrum showed an intense band peaking at ~16 500 cm^{-1} and a weaker band (more intense in ethanol than in acetonitrile) located at ~25 000 cm^{-1}, with total fluorescence quantum yields of 0.043 and 0.088 in acetonitrile and ethanol, respectively (Table 2). The excitation spectrum monitored at the main emission band almost matched the absorption spectrum, and the lower-energy band showed an unusually large Stokes shift with respect to the excitation spectrum. The excitation spectrum recorded at the maximum of the higher-energy emission band (25 000 cm^{-1}) was located at about the same position as that of the excitation spectrum monitored at the lower-energy emission band. The fluorescence decay was monitored at 16 670 and 21 740 cm^{-1} under excitation at 26 810 cm^{-1} (Table 4). A decay time of 3.6−4.5 ns, together with a second decay time of 1.8 ns, was obtained in acetonitrile. The first decay component showed a higher contribution at high wavenumbers, whereas the second component had a higher contribution at low wavenumbers. A minor third decay time of 0.24 ns (2%) was also detected at 21 740 cm^{-1}. The fluorescence decay was biexponential in ethanol. When monitored at 21 740 cm^{-1}, the main component of the fluorescence decay had a decay time of 4.88 ns, a minor decay time of 0.19 ns (5%) being also detected. At $\tilde{\nu}_{em} = 16\,670$ cm^{-1}, decay times of 2.59 ns (78%) and 4.47 ns (22%) were observed.

The fluorescence spectra of **2** in neutral aqueous solution of pH_c 7.00 with 40% ethanol showed similar features as those observed in acetonitrile and ethanol (part c of Figure 4), except for the fact that the lower-energy emission band was broader than that observed in acetonitrile and ethanol, with a strong shoulder in the 20 000 cm^{-1} region (absent in the nonaqueous solvents) being clearly observed. Also, the higher-energy emission band (~25 000 cm^{-1}) was weaker than those in the other two solvents. The total fluorescence quantum yield was measured to be 0.100 (Table 2). The fluorescence decay was biexponential in the range 16 390−20 410 cm^{-1} under excitation at 26 810 cm^{-1} (Table 4), with a decay time of 3.0 ns (with

TABLE 4: Fluorescence Decay Times τ and Associated Percentages (in Parentheses) of 2 in Various Solvents at 298 K; Shown in Brackets Are the Species to Which Each Decay Time Was Assigned

solvent	$\tilde{\nu}_{exc}$/cm^{-1}	$\tilde{\nu}_{em}$/cm^{-1}	τ_1/ns	τ_2/ns	τ_3/ns	χ^2
			neutral media			
acetonitrile	26 810	21 740	4.48 ± 0.09 (14%) [$\mathbf{N}^*_{anti}$]	1.79 ± 0.09 (84%) [**T***]	0.237 ± 0.013 (2%)[a]	1.020
	26 810	16 670	3.60 ± 0.09 (11%) [$\mathbf{N}^*_{anti}$]	1.721 ± 0.007 (89%) [**T***]		1.066
ethanol	26 810	21 740	4.881 ± 0.006 (95%) [$\mathbf{N}^*_{anti}$]	0.187 ± 0.003 (5%)[a]		1.271
	26 810	16 670	4.47 ± 0.11 (22%) [$\mathbf{N}^*_{anti}$]	2.59 ± 0.02 (78%) [**T***]		0.961
aqueous solution	26 810	20 410	6.90 ± 0.03 (63%) [**A***]	2.99 ± 0.03 (37%) [**T***]		1.078
(pH_c 7.00, 40% EtOH)	26 810	18 180	6.84 ± 0.07 (29%) [**A***]	3.052 ± 0.015 (71%) [**T***]		1.092
	26 810	16 390	6.47 ± 0.15 (12%) [**A***]	2.954 ± 0.012 (88%) [**T***]		1.081
			basic media			
aqueous solution	29 850	20 000	7.078 ± 0.006 [**A***]			1.185
(pH_c 13, 40% EtOH)	29 850	19 230	7.084 ± 0.007 [**A***]			1.111
			acid media			
acetonitrile	26 810	22 730	13.393 ± 0.015 (95%) [**C***]	1.97 ± 0.04 (5%)[a]		1.080
($[HClO_4] = 1.5 \times 10^{-3}$ mol dm^{-3})	26 810	19 610	13.501 ± 0.019 (90%) [**C***]	2.63 ± 0.03 (10%)[a]		1.058
ethanol	26 810	22 220	0.485 ± 0.004 (47%) [**C***][b]	3.343 ± 0.015 (40%) [**T***]	0.124 ± 0.003 (13%) [**C***][b]	1.045
(pH_c 1.40)	26 810	17 240	0.323 ± 0.002 (—)[c] [**C***][b]	2.841 ± 0.002 (—)[c] [**T***]		1.087
aqueous solution	26 810	17 860	1.12 ± 0.02 (11%)[a]	2.984 ± 0.007 (89%) [**T***]		1.040
(pH_c 1.50, 40% EtOH)	26 810	16 670	1.34 ± 0.05 (8%)[a]	2.936 ± 0.008 (92%) [**T***]		1.081

[a] Decay time probably due to an impurity. [b] Decay time associated with the decay of **C***, nonexponential due to geminate recombination of the fragments after photodissociation. [c] The percentages cannot be calculated because the associated amplitude of the short lifetime is negative.

higher contribution at low wavenumbers) and a second decay time of 6.5−6.9 ns (with higher contribution at high wavenumbers).

Basic Media. The excitation and emission spectra of **2** in aqueous solution of pH_c 13.00 with 40% ethanol (part d of Figure 4) were independent of the monitoring wavenumbers. The emission spectrum of **2** showed only one band located at about 20 000 cm^{-1} with a fluorescence quantum yield of 0.229 (Table 2). The fluorescence excitation spectrum overlapped the emission spectrum and showed a reasonable agreement with the absorption spectrum obtained under the same acidity conditions. The fluorescence decay of **2** was monoexponential (Table 4) with a decay time of 7.1 ns. No fluorescence was however detected for **1** under basic conditions.

Acidified Media. In acidified acetonitrile, a single emission band (maximum at ∼24 000 cm^{-1}) with a fluorescence quantum yield of 0.371 (Table 2) was detected for **1** (part a of Figure 5). The excitation spectrum, which showed a good agreement with the absorption spectrum in the first absorption band region, overlapped the emission band, and both spectra were independent of the monitoring wavenumbers. The fluorescence decay was monoexponential with a decay time of 2.30 ns (Table 3).

The fluorescence spectra of **1** were also recorded in aqueous solution of pH_c 0.49 with 40% ethanol (part b of Figure 5). The excitation spectrum almost coincided with the absorption band measured under the same acidity conditions, and showed no dependence on the monitoring emission wavenumber. The emission spectrum had a single emission band, which was independent of the monitoring excitation wavenumber and showed an anomalously large Stokes shift with respect to the excitation spectrum. This emission band was analogous to the main fluorescence band observed in neutral medium, and showed a fluorescence quantum yield of 0.168. The fluorescence decay was monoexponential at 22 730 cm^{-1} with a decay time of 1.74 ns (Table 3), becoming biexpoential at 20 830 cm^{-1} with a decay time of 1.73 ns and a minor component (6%) of 6.1 ns.

In acidified ethanol (part c of Figure 5), dual fluorescence was observed for **1**. The spectrum showed an intense band at

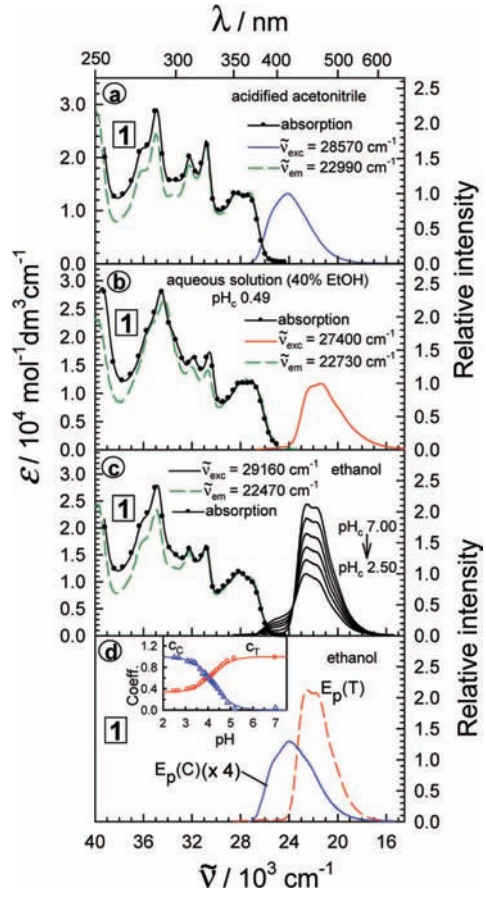

Figure 5. Absorption and normalized fluorescence excitation and emission spectra of **1** in (a) acidified acetonitrile, $[HClO_4] = 1.3 \times 10^{-3}$ mol dm^{-3} (b) aqueous solution (with 40% ethanol) of pH_c 0.49, and (c) ethanol at various pH_c values between 2.50 and 7.00. (d) Pure fluorescence spectra of **C*** and **T*** in ethanol obtained applying principal component global analysis to the series of fluorescence spectra plotted in part in panel (c). The coefficients c_C and c_T representing the contributions of **C*** (Δ) and **T*** (○) emission at each pH_c are shown in the inset, together with the fit of eqs 2 and 3 to these coefficients (solid lines).

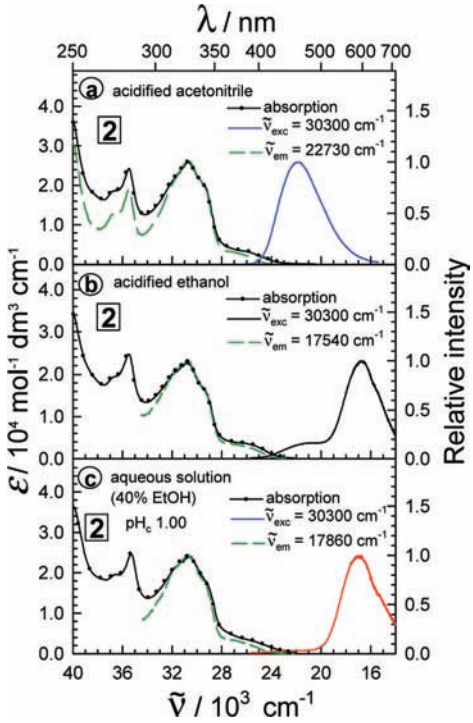

Figure 6. Normalized fluorescence excitation and emission spectra of **2** in (a) acidified acetonitrile, $[HClO_4] = 1.5 \times 10^{-3}$ mol dm^{-3}; (b) acidified ethanol, $pH_c = 1.4$; and (c) aqueous solution (with 40% ethanol) of pH_c 1.00, together with the absorption spectra in the same solvents.

22 600 cm^{-1}, similar to that detected in neutral media, accompanied by a weak shoulder at about the same position as that of the emission band obtained in acidified acetonitrile. The excitation spectrum was independent of the monitoring emission wavenumber and overlapped the weak emission band, showing a good coincidence with the absorption spectrum. The total fluorescence quantum yield was measured to be 0.332. The fluorescence decay was biexponential between 21 740 and 25 640 cm^{-1} with a decay time of 1.7 ns, similar to that recorded in neutral ethanol, and a second decay time of 0.41−0.68 ns (Table 3). The amplitude of the short decay time decreased as the emission wavenumber decreased, becoming negative at 21 740 cm^{-1}, whereas that of the long decay time increased as the emission wavenumber decreased.

The fluorescence spectra of **2** were recorded in acidified acetonitrile (part a of Figure 6). The excitation and emission spectra were independent of the monitoring wavenumbers. The emission spectrum showed only one band (at ∼22 000 cm^{-1}, fluorescence quantum yield 0.226). The excitation spectrum, which almost coincided with the absorption spectrum, showed an intense band at ∼30 700 cm^{-1} and a shoulder at ∼ 26 000 cm^{-1} that overlapped the emission band. The fluorescence decay was biexponential both at 22 730 and 19 610 cm^{-1} with a main decay time of 13.4 ns and a minor second component of 2.0−2.6 ns (Table 4).

In acidified ethanol, the excitation and emission spectra of **2** (part b of Figure 6) were independent of the monitoring wavenumbers. The excitation spectrum, which was very similar to that measured in acidified acetonitrile, almost matched the absorption spectrum. The emission spectrum showed two bands. The most intense band, with maximum at 16 600 cm^{-1}, was very similar to the lower-energy emission band detected in neutral ethanol, and the weaker band, peaking at ∼22 000 cm^{-1}, was located at about the same position as that of the emission band recorded in acidified acetonitrile and overlapped the weak shoulder of the excitation spectrum. The total fluorescence quantum yield was 0.076. The fluorescence decay was biexponential at 17 240 cm^{-1} with a decay time of 2.84 ns, very similar to one of the decay times measured in neutral ethanol, and a second decay time of 0.32 ns, with negative amplitude (Table 4). The fluorescence decay was triexponential at 22 220 cm^{-1} with decay times of 0.49, 3.34, and 0.12 ns.

The excitation and emission spectra of **2** in aqueous solution of pH_c 1.00 with 40% ethanol (part c of Figure 6) were independent of the monitoring wavenumbers. The excitation spectrum, which almost coincided with the absorption spectrum, was analogous to those observed in acidified acetonitrile and ethanol. The emission spectrum showed, except for a slight emission at ∼22 000 cm^{-1}, only one band which did not overlap the excitation spectrum (maximum at 16 700 cm^{-1}, fluorescence quantum yield 0.057). The fluorescence decay in aqueous solution (pH_c 1.5, 40% ethanol) was biexponential both at 16670 and 17860 cm^{-1} (Table 4) with a main component of 2.94−2.98 ns decay time and a minor component of 1.1−1.3 ns.

Discussion

1. Interpretation of the Absorption Spectra of 1 and 2 in Various Solvents: Acid−Base and Tautomeric Equilibria in the Ground State. The observed red shift of the absorption spectrum of **2** and **1** in aqueous solution with 40% ethanol (parts a and c respectively of Figure 1) on both increasing and decreasing pH_c from neutral conditions, together with the presence of isosbestic points, indicate the existence of two acid−base equilibria involving protonation (acidity constant K_{a1}) and deprotonation (acidity constant K_{a2}) of **1** and **2**. We applied principal component global analysis[38,39] (PCGA) to the series of absorption spectra, as described previously for HBI.[39] The method provides the calculated pure spectra of the protonated ($\mathbf{A}_p$), neutral ($\mathbf{A}_n$) and deprotonated ($\mathbf{A}_d$) forms (parts b and d of Figure 1), together with their experimental and calculated acidity-dependent spectral contributions[39] c_p, c_n, and c_d (insets in parts b and d of Figure 1), and the pK_{a1} and pK_{a2} values (Table 5). The calculated absorption spectrum of the protonated form, $\mathbf{A}_p$, must correspond to the monocation protonated at the benzimidazole N3, as this should be the more basic position of **1** and **2**, in analogy with related species.[27,31] Similarly, the spectrum of the deprotonated form, $\mathbf{A}_d$, must be due to the anion dissociated at the hydroxyl group, the more acidic site of these molecules. The calculated pK_{a1} values (3.04 for **1** and 3.71 for **2**) were much lower than those of both the related molecule HBI (5.48)[27] and benzimidazole (5.53),[40] this indicating that the naphthol substituent at the benzimidazole C2 decreases the basicity at the benzimidazole N3. However, the pK_{a2} values (9.49 for **1** and 9.97 for **2**) were similar to those reported[41] for the deprotonation of 1-naphthol (9.23) and 2-naphthol (9.49).

In ethanol, the absorption spectrum of **1** shifted to the red as the acidity increased (part a of Figure 2), and several isosbestic points appeared, indicating that protonation of the neutral form is taking place. PCGA,[38,39] applied to the series of absorption spectra, provided the calculated pure spectra of the protonated and neutral forms ($\mathbf{A}_p$ and $\mathbf{A}_n$, part b of Figure 2), together with their experimental and calculated acidity-dependent contributions[42] c_p and c_n (inset in part b of Figure 2) and the pK_{a1} (Table 5). A good agreement between the experimental and calculated coefficients was observed and the calculated absorption spectra $\mathbf{A}_p$ and $\mathbf{A}_n$ coincided with the experimental absorption spectra measured at pH_c 1.13 and 7.00, respectively. The spectrum obtained in acid media corresponds, as previously discussed, to the monocation **C**, protonated at the benzimidazole N3.

TABLE 5: Acidity Constants K_{a1} and K_{a2} of 1 and 2, Estimated Tautomeric Equilibrium Constant K of 1, and Rate Constants k_C and k_{CT} Obtained for 1, in Various Solvents at 298 K[a]

	2		1				
solvent	pK_{a1}	pK_{a2}	pK_{a1}	pK_{a2}	K	$k_C/10^9$ s^{-1}	$k_{CT}/10^9$ s^{-1}
aqueous solution (40% EtOH)	3.71 ± 0.03	9.97 ± 0.02	3.038 ± 0.005	9.486 ± 0.006	0.22		
ethanol			4.215 ± 0.010[b] 4.073 ± 0.016[c]		∼0	0.78	1.0
ethylene glycol					0.08		
glycerol					0.30		

[a] The equilibrium constants are estimated as molar concentration quotients. [b] From fluorescence spectra. [c] From absorption spectra.

It is observed in part d of Figure 1 and part b of Figure 2 that the spectrum $\mathbf{A}_p$ of the cation of **1** showed similar values of the maximum molar absorption coefficient at the first absorption band in aqueous solution with 40% ethanol (1.3×10^4 mol^{-1} dm^3 s^{-1}) and in pure ethanol (1.4×10^4 mol^{-1} dm^3 s^{-1}). Nevertheless, for the neutral form (spectrum $\mathbf{A}_n$), this value was in aqueous solution with 40% ethanol (1.3×10^4 mol^{-1} dm^3 s^{-1}) rather lower than that obtained in ethanol (1.8×10^4 mol^{-1} dm^3 s^{-1}). Besides that, the spectrum of the neutral form of **1** in aqueous solution with 40% ethanol showed a lower-energy band (band II, ∼25 000 cm^{-1}) absent in ethanol and aprotic solvents. In view of this, we measured the spectra of this compound in ethanol/water mixtures, with a v/v ethanol content ranging from 40 to 100% (part c of Figure 2). It was observed that absorption band II decreased with the ethanol content, whereas that of band I increased, and several isosbestic points were detected. Furthermore, absorption band II was also observed in ethylene glycol and glycerol (part d of Figure 2), its proportion with respect to band I increasing in the order ethanol < ethylene glycol < glycerol, and several isosbestic points were also detected. These results seem to indicate that, in these solvents and in neutral aqueous solution with 40% ethanol, an equilibrium exists between two neutral forms. A tautomeric equilibrium was reported by us for the related molecules 2-(3′-hydroxy-2′-pyridyl)benzimidazole, HPyBI,[30] and 2-(2′-hydroxyphenyl)benzimidazole, HBI,[27] which showed in aqueous solution a higher-energy absorption band (band I) due to the normal form and a lower-energy band (band II) attributed to the tautomer **T**.

To elucidate if absorption bands I and II of **1** originate, as for HBI and HPyBI, from two different tautomers in the ground state, we performed ab initio B3LYP calculations at the 6-31G** level on the ground-state $\mathbf{N}_{syn}$ and $\mathbf{N}_{anti}$ rotamers and the tautomer **T** of **1** (Chart 2), both in the gas phase and in water (with the PCM continuum model). The three forms were planar, and the results in Table 1 indicate that the $\mathbf{N}_{syn}$ rotamer is the most stable form in the ground state (both in the gas phase and in water), followed by **T**, whereas the rotamer $\mathbf{N}_{anti}$ is more unstable than **T**. The dipole moment increased in the series $\mathbf{N}_{syn}$ < $\mathbf{N}_{anti}$ < **T**. This fact explains that the energy difference between **T** and $\mathbf{N}_{syn}$ (and to a lesser extent that between $\mathbf{N}_{anti}$ and $\mathbf{N}_{syn}$) gets significantly smaller on going from gas phase to aqueous solution. These results indicate that the absorption band II of **1** appearing in water might be due to the tautomer **T**, as found for the related molecules HPyBI[30] and HBI.[27] The spectra in different solvents reveal however that the tautomerism (and probably the rotamerism) of this molecule is not only controlled by the polarity of the solvent but also by specific solvent effects. In fact, if we compare the absorption spectra of neutral **1** in protic and aprotic solvents of the same dielectric permittivity, for example ethylene glycol (37.70) and acetonitrile (35.94), we see that absorption band II was observed only in the protic solvent ethylene glycol (part d of Figure 2 for the alcohol, and part b of Figure 3 for acetonitrile). This indicates that specific solvent effects are crucial to stabilize tautomer **T**, probably with the hydrogen-bond donor ability of the solvent (very high for water and glycerol) being a key solvent property. Similar results were obtained by us in an experimental and theoretical study of the related molecule 4,5-dimethyl-2-(2′-hydroxyphenyl)imidazole.[43]

From the above discussion, we propose that absorption bands I and II of **1** correspond respectively to the neutral form **N** and its tautomer **T** (Chart 2). The fluorescence measurements of **1**, discussed in the next section, provide more evidence supporting this interpretation of the results and will allow us to establish the identity of the neutral **N** rotamers responsible for absorption band I. An estimation of the equilibrium constant $K = [\mathbf{T}]/[\mathbf{N}]$ can be made assuming that 1) the spectrum of **1** in neutral ethanol, where only **N** is present, is similar to the spectrum of **N** in aqueous solutions and other alcohols, and 2) that, at 27 700 cm^{-1} (absorption maximum of **N**), **T** does not absorb significantly. Under these approximations, the ratio between the molar absorption coefficient of **N**, ε_N, at 27 700 cm^{-1} (band I) in any alcohol showing equilibrium between **N** and **T**, and the value of ε_N in ethanol at the same wavenumber, allows the equilibrium molar fraction of **N** to be estimated. The equilibrium constants obtained in this way are shown in Table 5. It is seen that K increased in the series ethanol < ethylene glycol < glycerol. The equilibrium constant in pure water could not be determined due to the low solubility of **1**, but the value should be higher than that estimated in aqueous solution with 40% ethanol (0.22).

It is noteworthy that no evidence of the existence of **T** in the ground state was obtained for **2**, the absorption spectra being very similar in all of the solvents studied (parts a−c of Figure 4). This result exemplifies the fact that subtle changes in molecular structure may have a profound effect on the tautomeric and rotameric equilibria.

2. Interpretation of the Fluorescence Spectra and Lifetimes of 1 and 2 in Neutral Solutions: ESIPT and Ground-State Tautomeric and Conformational Equilibrium. From the fluorescence spectra of **1** in neutral solutions (Figure 3), it is observed that excitation at band I, assigned to **N**, led to an emission spectrum with a large Stokes shift with respect to the excitation band in all of the solvents studied, clearly indicating that the emission is not due to **N***. Furthermore, the spectra were very similar in all of the solvents, except for the disappearance of structure on going from cyclohexane to water and for the fact that in all of the solvents but cyclohexane the main fluorescence band was accompanied at certain excitation wavenumbers by a weak emission at ∼26 000 cm^{-1}. These results suggest that the main fluorescence is caused by the same species in all of the solvents studied. In water, where **N** and **T** coexist in the ground state, excitation at band II (due to **T**) led to an emission band overlapping the excitation band (part d of

Figure 3), indicating that **T*** is the fluorescent species responsible for the emission at 22 100 cm^{-1}. Moreover, the emission spectrum of **T*** coincided, except for the weak band at ~26 000 cm^{-1}, with the emission band obtained under the excitation of **N** at band I, indicating that **N** undergoes in the excited state an intramolecular proton transfer from the hydroxyl group to the benzimidazole N3 to give **T***, as previously reported for related molecules.[27,29,30,43,44] This ESIPT process also occurs in cyclohexane, acetonitrile, and ethanol, as in all of these solvents excitation of **N** led to an emission spectrum very similar to that of **T*** in aqueous solution with 40% ethanol (Figure 3). Therefore, the fluorescence decay times of 1.44−1.70 ns (Table 3) measured in all of these solvents correspond to **T***. Furthermore, the fact that within our time resolution (~0.1 ns) no formation of **T*** from **N*** was detected indicates that the ESIPT is ultrafast and therefore that **N** exhibits already in the ground state an intramolecular hydrogen bond between the OH group and the benzimidazole N3, and therefore, **N** is in the planar syn conformation $\mathbf{N_{syn}}$ (Chart 2).

The fluorescence of **1** in acetonitrile, ethanol, and water (parts b−d of Figure 3) showed a weak higher-energy emission, located at the position where fluorescence from **N*** would be expected, together with the fluorescence from **T***. This fact reveals that in these solvents there is a small fraction of ground-state **N** molecules without the intramolecular hydrogen bond N···H−O, unable therefore to yield **T*** upon excitation. Moreover, the excitation spectrum monitored at the higher-energy emission band was located at the same position as that assigned to $\mathbf{N_{syn}}$. This fact leads us to propose that the minor amount of **N** molecules giving **N*** fluorescence show also a planar structure, probably the anti structure $\mathbf{N_{anti}}$ (Chart 2), as found for the structurally related molecule HBI in protic solvents.[27] We have to point out here that the proportion of ground-state **N** conformers of **1** other than $\mathbf{N_{syn}}$ seems to be however very small both in protic and aprotic solvents, as the excitation spectrum of the **T*** emission practically coincided with the absorption spectrum in the first absorption band region (at least with the same accuracy as in cyclohexane, a solvent where only $\mathbf{N_{syn}}$ exists in the ground state). Because of the weakness of the $\mathbf{N^*_{anti}}$ emission, its fluorescence decay time could only be measured in water, a value of 4.7 ns being obtained (Table 3).

From the previous discussion, we arrive at the following conclusions for the behavior of **1** in neutral solutions:

a) In cyclohexane, only the $\mathbf{N_{syn}}$ conformer was detected in the ground state, giving the fluorescent tautomer species **T*** upon excitation and ESIPT.

b) In acetonitrile and ethanol, $\mathbf{N_{syn}}$ and **T*** were also the main species detected in the ground and the excited state respectively, but a small fraction of $\mathbf{N_{anti}}$ molecules was also detected by its blue-shifted fluorescence.

c) In aqueous solution with 40% ethanol, a ground-state rotameric and tautomeric equilibrium between $\mathbf{N_{syn}}$, $\mathbf{N_{anti}}$, and **T** exists, with fluorescence from $\mathbf{N^*_{anti}}$ and **T*** being observed (Scheme 1). Ground-state **T** was only detected in water, and the amount of the minor conformer $\mathbf{N_{anti}}$ was also higher is aqueous solution than in other solvents.

The main general features of the fluorescence spectra of **2** (Figure 4) parallel those observed for **1**, this suggesting that isomer **2** undergoes also an ESIPT process. In agreement with the results of Douhal et al.,[33] dual fluorescence was observed for **2** in acetonitrile and ethanol (parts a and b of Figure 4), the spectra showing a higher-energy emission band, due to the normal form **N***, and a more intense lower-energy emission band

SCHEME 1: Excitation and Deactivation Pathways of 1 in Neutral Aqueous Solution with 40% Ethanol

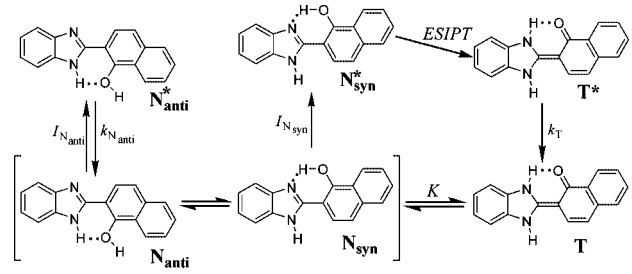

originated by **T***. The excitation spectra monitored at the **T*** emission band must correspond to the planar syn rotamer $\mathbf{N_{syn}}$, whereas that obtained at the **N*** emission band must be due to the **N** rotamers without the intramolecular hydrogen bond N···H−O (unable to undergo ESIPT), probably the planar anti rotamers $\mathbf{N_{anti}}$ (Chart 2). The fact that the excitation spectrum of $\mathbf{N_{syn}}$ almost matched the absorption spectrum (specially in acetonitrile) indicates that the amount of $\mathbf{N_{anti}}$ rotamers must be very small compared to that of $\mathbf{N_{syn}}$.

The fluorescence decay of **2** was measured in acetonitrile and ethanol at 16 670 cm^{-1} (emission band of **T***) and at 21 740 cm^{-1}. In acetonitrile, a main component of decay time of 1.72−1.79 ns (>80%, Table 4), which must be due to **T***, and a minor component of 3.60−4.48 ns, which must correspond to $\mathbf{N^*_{anti}}$, were obtained. These values are in good agreement with those previously reported by Douhal et al.[33] in the same solvent (1.68 and 4.88 ns, respectively). In ethanol, solvent where the contribution of $\mathbf{N^*_{anti}}$ emission was higher than in acetonitrile, a main decay time of 4.88 ns, due to $\mathbf{N^*_{anti}}$, was measured at 21 740 cm^{-1}, accompanied by a minor component (5%) of ~0.2 ns (also observed in acetonitrile) probably due to an impurity. At 16 670 cm^{-1}, the fluorescence decay was biexponential with a main decay time of 2.59 ns, due to **T***, and a second decay time (22%) of 4.47 ns that must correspond to $\mathbf{N^*_{anti}}$.

The fluorescence spectra of **2** in neutral aqueous solution with 40% ethanol (part c of Figure 4) showed some similarities with those recorded in acetonitrile and ethanol. The emission spectrum exhibited a weak band at ~27 000 cm^{-1}, which must be originated by $\mathbf{N^*_{anti}}$, and an intense band at lower wavenumbers that, as previously discussed, must correspond to **T***. The excitation spectrum recorded at the $\mathbf{N^*_{anti}}$ emission band was very similar to that recorded in acetonitrile and ethanol under similar conditions, and we likewise attribute it to $\mathbf{N_{anti}}$. In contrast to the behavior of **1** in neutral aqueous solution with 40% ethanol, for which the tautomer was in equilibrium with $\mathbf{N_{syn}}$ and $\mathbf{N_{anti}}$ in the ground state, no tautomer was detected for **2** in the ground state. The excitation spectrum monitored at the **T*** emission band did not overlap the emission spectrum of **T*** and was very similar to that of $\mathbf{N_{syn}}$ in acetonitrile and ethanol, and therefore must be originated only by $\mathbf{N_{syn}}$. On the other hand, the emission spectrum of **2** showed a broad shoulder at about 20 000 cm^{-1}, which was not detected in nonaqueous solvents, indicating that, besides $\mathbf{N^*_{anti}}$ and **T***, a third fluorescent component is present in neutral aqueous solution with 40% ethanol. On the basis of the fact that the acidity of the hydroxyl group at the naphthol ring increases upon excitation,[19] we propose that a fraction of $\mathbf{N_{anti}}$ rotamers dissociate in the excited state at the hydroxyl group yielding the anion **A*** (Scheme 2), as previously reported by us for HBI and derivatives.[27,44] To check this, we recorded the fluorescence spectra of **2** in aqueous solution of pH_c 13.00 with 40% ethanol (part d of Figure 4), conditions where only the anion **A** exists in the ground state. It is observed that the

SCHEME 2: Excitation and Deactivation Pathways of 2 in Neutral Aqueous Solution with 40% Ethanol

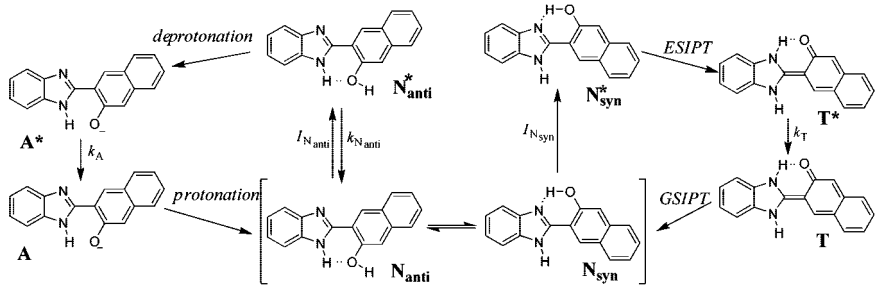

A* emission band showed its maximum at ~20 000 cm^{-1}, this being in agreement with the position where the emission shoulder, attributed to **A***, is detected in neutral aqueous solution with 40% ethanol.

The fluorescence decay of **2** in neutral aqueous solution with 40% ethanol was biexponential (Table 4) between 20 410 and 16 390 cm^{-1}, a spectral region where both **A*** and **T*** fluoresce. A decay time of 3.0 ns, with maximum contribution at low wavenumbers, due to **T***, was obtained. In agreement with our interpretation of the results, the second decay time value, 6.5−6.9 ns, was virtually coincident with that obtained for **A*** in basic aqueous solution with 40% ethanol (7.08 ns, Table 4) and contributed to the decay mainly at 20 410 cm^{-1}, a region where **A*** strongly fluoresces.

From the above results, we propose the mechanism of Scheme 2 to explain the behavior of **2** in neutral aqueous solution with 40% ethanol. A ground-state rotameric equilibrium between $\mathbf{N_{syn}}$ and $\mathbf{N_{anti}}$ was detected. Upon excitation, $\mathbf{N^*_{syn}}$ undergoes ESIPT to yield **T***, and $\mathbf{N^*_{anti}}$ partially deprotonates at the hydroxyl group to give **A***, which has a higher fluorescence quantum yield (Table 2). The fluorescence from $\mathbf{N^*_{anti}}$, **A***, and **T*** was observed. In acetonitrile and ethanol, $\mathbf{N^*_{anti}}$ does not dissociate, and only fluorescence from $\mathbf{N^*_{anti}}$ and **T*** was observed.

We must point out here that, for **1**, deprotonation of $\mathbf{N^*_{anti}}$ at the hydroxyl group to give the excited anion **A*** might also take place in neutral aqueous solution, but we do not have any experimental evidence of this process because **A*** is not fluorescent for this compound. Nevertheless, if this process would exist, it could not be very efficient, as the fluorescence quantum yield of **1** in neutral aqueous solution with 40% ethanol is of the same order of magnitude as in other solvents (Table 2).

Despite the fact that the absorption spectrum of **2** in any solvent is virtually due to $\mathbf{N_{syn}}$, which in the excited state rapidly converts to **T***, the fluorescence quantum yields of **T*** emission could not be obtained for this compound in any solvent. The reason for this is that emission from **T*** was always accompanied by that of $\mathbf{N^*_{anti}}$ (and also of **A*** in aqueous solution), and its contribution could not be subtracted from the total fluorescence because the pure emission spectrum of $\mathbf{N^*_{anti}}$ is unknown. However, we can say that the fluorescence quantum yield of the **T*** emission must be in any solvent markedly lower for **2** than for **1** because the total fluorescence quantum yields of **2** (due to $\mathbf{N^*_{anti}}$ and **T*** emissions in nonaqueous solvents and to $\mathbf{N^*_{anti}}$, **A***, and **T*** in aqueous solution with 40% ethanol) were in any solvent lower than the values of the yields of **T*** emission for **1** (Table 2). In acetonitrile, a solvent in which $\mathbf{N^*_{anti}}$ showed a minor contribution to the total fluorescence, the tautomer fluorescence quantum yield of **2** must be only slightly lower than the measured total fluorescence quantum yield (0.043, Table 2), and this value is about six times lower than that observed for **1**. In ethanol, the total fluorescence quantum yield was higher than that obtained in acetonitrile, probably due to the fact that the contribution of $\mathbf{N^*_{anti}}$ emission increased in this protic solvent. Furthermore, an even higher total fluorescence quantum yield was obtained in aqueous solution with 40% ethanol, because in this solvent the emission was mainly due to **A*** and **T***, and the fluorescence quantum yield of **A*** (0.229, Table 2), measured at pH_c 13.00, was much higher than that of the **T*** emission.

Finally, it is interesting to compare the absorption and emission characteristics of **1** and **2**. The $\mathbf{N^*_{anti}}$ emission maxima were similar for both compounds, and also the absorption maxima of $\mathbf{N_{syn}}$ and $\mathbf{N_{anti}}$ were for **1** and **2** very alike. The **T*** emission maximum is however markedly more red-shifted for **2** (~16 500 cm^{-1}) than for **1** (~22 000 cm^{-1}), indicating a much lower S_1-S_0 energy difference of **T*** for **2** than for **1**.

3. Interpretation of the Fluorescence Spectra and Lifetimes of 1 and 2 in Acidic Conditions: Solvent-Modulated Photodissociation of C* to Yield T*. The excitation spectra of **1** and **2** in acidified acetonitrile, ethanol, and water (Figures 5 and 6) almost coincided with the absorption spectra recorded in the same solvents under similar acidity conditions, previously attributed to the cation **C**, and therefore we assign them to the same species. For **1**, excitation of **C** in acetonitrile led to an emission band (part a of Figure 5), which overlapped its excitation spectrum and was independent of the monitoring wavenumber, indicating that **C*** is the emissive species (fluorescence quantum yield 0.371, Table 2). In agreement with this, the fluorescence decay was monoexponential with a decay time of 2.30 ns (Table 3).

The behavior of **2** in acidified acetonitrile is similar to **1** (part a of Figure 6). The emission spectrum overlaps the absorption spectrum of **C**, which indicates that **C*** is also the fluorescent species with a quantum yield of 0.226 (Table 2). The fluorescence decay was biexponential in acetonitrile (Table 4) with a main decay time of 13.4 ns (≥90%), due to **C***, and a minor decay time of 2.0−2.6 ns, which might be due to an impurity.

In acidified aqueous solution with 40% ethanol, the emission spectra of **1** and **2** showed a large Stokes shift independently of the monitoring excitation wavenumber (part b of Figure 5 and part c of Figure 6), this suggesting that they correspond to a species different from **C***. In addition, the emission spectrum of **1** was essentially the same as that obtained in neutral aqueous solution with 40% ethanol (part d of Figure 3) under excitation at band II, attributed to **T***, whereas that of **2** was very similar to the lower-energy emission band, due to **T***, observed in neutral solutions (Figure 4). This means that for both isomers **C*** deprotonates at the hydroxyl group to give **T***, the process being very fast as no emission from **C*** was detected. Furthermore, the fluorescence quantum yield measured for **1** (0.168) was about the same as that obtained for the **T*** emission in neutral aqueous solution with 40% ethanol (0.145), whereas the value obtained for **2** (0.057) was of the same order of the estimated fluorescence quantum yield of **T*** emission in neutral

SCHEME 3: Excitation and Deactivation Pathways of 1 in Acidified Ethanol; a Similar Mechanism Holds for 2

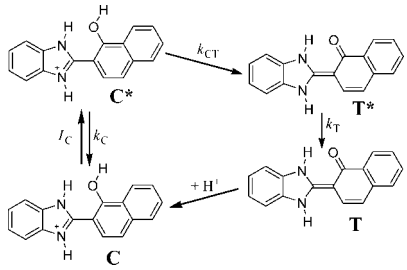

acetonitrile (~0.043, total fluorescence quantum yield due to $\mathbf{N}^*_{anti}$ and **T*** emission, but with a very low contribution of $\mathbf{N}^*_{anti}$ to the total emission). In agreement with this interpretation, the fluorescence decay of **1** and **2** in acidified aqueous solution with 40% ethanol showed decay times of 1.73 ns for **1** and 2.96 ns for **2**, these values coinciding with those measured for **T*** under neutral conditions (1.70 ns for **1** and 3.00 ns for **2**, Tables 3 and 4). A second decay time, with a very low contribution, was detected for both compounds and is probably due to an impurity.

In acidified ethanol, dual fluorescence was observed under excitation of **C** for both **1** and **2** (part c of Figure 5 and part b of Figure 6), the spectra being independent of the excitation wavenumber. For both isomers, the strong band was very similar to that of **T*** in neutral ethanol and must correspond to **T***, whereas the fact that the weak band both overlapped the excitation band of **C** and was located at about the same position as that of **C*** in acetonitrile suggests that this emission corresponds to **C***. This indicates that, for both **1** and **2**, a fraction of **C*** molecules deprotonate at the hydroxyl group to give **T***, as depicted in Scheme 3. Despite the fact that photodissociation leads to a nonexponential decay of the photoacid due to geminate recombination of the fragments,[19] we have fitted the fluorescence decay of **1** and **2** in acidified ethanol to a sum of exponential functions to identify the fluorescent species involved and get information on the global photodissociation process. The fluorescence decay of **1** (Table 3) could be reasonably fitted to a biexponential function with a decay time τ_1 (1.66−1.75 ns) coincident with that measured for **T*** in neutral ethanol (1.63−1.66 ns), and therefore it must correspond to **T***, and a second decay time (0.41−0.68 ns) that must correspond to **C***, its value being shorter than that of **C*** in acetonitrile (2.30 ns), a solvent in which deprotonation of **C*** does not occur. The amplitudes ratio a_2/a_1 was positive at 25 000 cm^{-1} and decreased with the emission wavenumber, becoming negative below 23 810 cm^{-1}. This clearly indicats that the species being excited, **C**, undergoes a transformation in the excited state. For **2**, the fluorescence decay in acidified ethanol could be fitted to a biexponential function at 17 240 cm^{-1}, whereas a triexponential function was needed at 22 220 cm^{-1}. A decay time of 2.8−3.3 ns, similar to that measured for **T*** in neutral ethanol, was observed at both emission wavenumbers, whereas the short decay times are related to the decay of **C***. At 17 240 cm^{-1}, the amplitude of the short decay time was negative, as a consequence of the excited-state transformation **C*** → **T***. The fact that photodissociation of **C*** takes place to a great extent in ethanol indicates that the monocations of **1** and **2** are strong photoacids. This property makes these compounds very suitable to study the dynamics of photodissociation processes in neat alcohols. Investigation on the detailed mechanism of proton transfer from the excited monocations of **1** and **2** to neat alcohols is currently in progress.

The emission spectra of **1** were recorded in ethanol between neutral and acidic conditions (part c of Figure 5). As the acidity increased from neutral conditions to pH_c 2.50, the emission from **T*** decreased, whereas that from **C*** increased. According to the proposed mechanism (Scheme 3), any fluorescence spectrum from the series should be the sum of the contributions of the spectra from **C*** and **T*** ($\mathbf{F_C}$ and $\mathbf{F_T}$, respectively), according to eqs 1−4,

$$F = c_C F_C + c_T F_T \tag{1}$$

$$c_C = \frac{[H^+]}{K_{a1} + [H^+]} \tag{2}$$

$$c_T = \frac{K_{a1} + \alpha[H^+]}{K_{a1} + [H^+]} \tag{3}$$

$$\alpha = \left(\frac{\varepsilon_C}{\varepsilon_N}\right)_{\bar{\nu}} \frac{k_{CT}}{k_C + k_{CT}} \tag{4}$$

In these equations, c_C and c_T represent the acidity-dependent contributions of **C*** and **T*** to any experimental spectrum, k_C and k_{CT} have the meaning shown in Scheme 3, and the ratio $(\varepsilon_C/\varepsilon_N)_{\bar{\nu}}$ represents the quotient between the molar absorption coefficients of **C*** and **N*** at the experimental excitation wavenumber, 29 150 cm^{-1} (as previously explained, **T*** is formed from $\mathbf{N}^*_{syn}$ in neutral media, $\mathbf{N_{syn}}$ being always the main ground-state conformer).

In agreement with the proposed mechanism, a principal component analysis of the spectral series indicated that two independent spectral components are needed to reproduce the fluorescence spectra of **1** in neutral-to-acid ethanol solutions. We then applied PCGA[39] to the spectral series to further test our model and to obtain the pure spectra $\mathbf{F_C}$ and $\mathbf{F_T}$ (part d of Figure 5), as well as their experimental and calculated contributions c_C and c_T (inset of part d of Figure 5) and the parameters pK_{a1} and α (Table 5). It is seen (part d of Figure 5) that the calculated spectrum $\mathbf{F_T}$ coincided with that measured for **T*** under neutral conditions (part c of Figure 3), whereas the calculated spectrum $\mathbf{F_C}$ very much resembled that measured for **C*** in acetonitrile (part a of Figure 5). Moreover, the optimized pK_{a1} (4.215 ± 0.010) was close to that provided by the analysis of the acidity dependence of the absorption spectra (4.073 ± 0.016). Furthermore, from the calculated α and taking into account that at the excitation wavenumber employed $(\varepsilon_C/\varepsilon_N)_{\bar{\nu}}$ is estimated to be 0.587, the ratio $k_{CT}/(k_C + k_{CT})$ was calculated to be 0.562. However, from the short decay times obtained in the spectral region where **C*** mainly fluoresces (0.682 and 0.435 ns, Table 3), an averaged τ_C value of 0.56 ns was estimated. From these values, and knowing that τ_C equals $(k_C + k_{CT})^{-1}$, the rate constants k_{CT} and k_C were estimated to be 1.0×10^9 and 7.8×10^8 s^{-1} respectively (Table 5).

Conclusions

We have studied in this work the ground- and excited-state behavior of 2-(1′-hydroxy-2′-naphthyl)benzimidazole, **1**, and 2-(3′-hydroxy-2′-naphthyl)benzimidazole, **2**, in various solvents. We have shown that whereas in apolar solvents these compounds exist in the ground state as the planar syn normal form $\mathbf{N_{syn}}$, with an intramolecular hydrogen bond N−H···O, in acetonitrile and ethanol a rotameric equilibrium between $\mathbf{N_{syn}}$, and a minor amount of its planar anti rotamer $\mathbf{N_{anti}}$ is established. In aqueous solution with 40% ethanol, a rotameric and tautomeric equilibrium between $\mathbf{N_{syn}}$, $\mathbf{N_{anti}}$, and **T** was observed for **1** in the ground state. This tautomer was also detected for **1** in

ethylene glycol and glycerol, its amount increasing with increasing hydrogen-bond donation ability of the solvent. For **2**, **T** was however not detected in the ground state in any of the solvents studied.

Excitation of $\mathbf{N_{syn}}$ led to an ultrafast ESIPT to yield **T*** in all of the solvents studied, with fluorescence from **T*** being observed. In nonaqueous solvents, excitation of $\mathbf{N_{anti}}$ (unable to undergo ESIPT) led to its own emission, but a fraction of $\mathbf{N_{anti}}$ molecules dissociated in the excited state in aqueous solution with 40% ethanol for **2**, as a result of the increased acidity of the hydroxyl group in the excited state, yielding the anion **A***. This dissociation process was not detected for **1**, whose anion is not fluorescent.

Protonation of **1** and **2** takes place at the benzimidazole N3 to give monocation **C**. Excitation of **C** in the aprotic solvent acetonitrile led for both compounds to fluorescence from **C***. In ethanol, a fraction of the cation molecules experienced a photodissociation process at the hydroxyl group due to the increased acidity of this group upon excitation and due to the higher basicity of ethanol compared to that of acetonitrile. The product of the photodissociation is the tautomer **T***, with dual fluorescence (from **C*** and **T***) being observed. In aqueous solution with 40% ethanol, deprotonation of **C*** is so fast for both **1** and **2** that fluorescence from **C*** was undetected.

The efficient excited-state deprotonation of the monocations of **1** and **2** in ethanol makes these compounds very good probes to unravel the mechanism of photodissociation in neat solvents.

Acknowledgment. We thank the Spanish Ministry of Education and Science and the European Regional Development Fund (project CTQ2007-68057-C02-01/BQU) and the Xunta de Galicia (Consellería de Innovación e Industria, project PGIDIT05-PXIC20905PN and INCITE08E1R209060ES grant) for financial support of our work. A. Brenlla thanks the Fundación Segundo Gil Dávila for a postgraduate research grant.

References and Notes

(1) Sobolewski, A. L.; Domcke, W. *ChemPhysChem* **2006**, *7*, 561.
(2) Meyer, T. J.; Huynh, M. H. V.; Thorp, H. H. *Angew. Chem., Int. Ed.* **2007**, *46*, 5284.
(3) Hosler, J. P.; Ferguson-Miller, S.; Mills, D. A. *Annu. Rev. Biochem.* **2006**, *75*, 165.
(4) *Hydrogen-Transfer Reactions*; Hynes, J. T., Klinman, J. P., Limbach, H. H., Schowen, R. L., Eds.; 2007; Vol. 1−4.
(5) Formosinho, S. J.; Arnaut, L. G. *J. Photochem. Photobiol., A* **1993**, *75*, 21.
(6) Ormson, S. M.; Brown, R. G. *Prog. React. Kinet.* **1994**, *19*, 45.
(7) Chen, K.-Y.; Hsieh, C.-C.; Cheng, Y.-M.; Lai, C.-H.; Chou, P.-T. *Chem. Commun.* **2006**, 4395.
(8) Park, S.; Kwon, O.-H.; Kim, S.; Park, S.; Choi, M.-G.; Cha, M.; Park, S. Y.; Jang, D.-J. *J. Am. Chem. Soc.* **2005**, *127*, 10070.
(9) Paterson, M. J.; Robb, M. A.; Blancafort, L.; DeBellis, A. D. *J. Phys. Chem. A* **2005**, *109*, 7527.
(10) Klymchenko, A. S.; Stoeckel, H.; Takeda, K.; Mely, Y. *J. Phys. Chem. B* **2006**, *110*, 13624.
(11) Rodembusch, F. S.; Leusin, F. P.; da Costa Medina, L. F.; Brandelli, A.; Stefani, V. *Photochem. Photobiol. Sci.* **2005**, *4*, 254.
(12) Yushchenko, D. A.; Shvadchak, V. V.; Klymchenko, A. S.; Duportail, G.; Pivovarenko, V. G.; Mely, Y. *J. Phys. Chem. A* **2007**, *111*, 8986.
(13) Sobolewski, A. L. *Phys. Chem. Chem. Phys.* **2008**, *10*, 1243.
(14) Ma, D.; Liang, F.; Wang, L.; Lee, S. T.; Hung, L. S. *Chem. Phys. Lett.* **2002**, *358*, 24.
(15) Gaenko, A. V.; Devarajan, A.; Tselinskii, I. V.; Ryde, U. *J. Phys. Chem. A* **2006**, *110*, 7935.
(16) Mansueto, E. S.; Wight, C. A. *J. Am. Chem. Soc.* **1989**, *111*, 1900.
(17) Silvi, S.; Arduini, A.; Pochini, A.; Secchi, A.; Tomasulo, M.; Raymo, F. M.; Baroncini, M.; Credi, A. *J. Am. Chem. Soc.* **2007**, *129*, 13378.
(18) Gutman, M.; Nachliel, E. *Annu. Rev. Phys. Chem.* **1997**, *48*, 329.
(19) Agmon, N. *J. Phys. Chem. A* **2005**, *109*, 13.
(20) Pérez-Lustres, J. L.; Rodríguez-Prieto, F.; Mosquera, M.; Senyushkina, T. A.; Ernsting, N. P.; Kovalenko, S. A. *J. Am. Chem. Soc.* **2007**, *129*, 5408.
(21) Waluk, J. *Conformational Analysis of Molecules in Excited States*; Wiley-VCH: New York, 2000.
(22) Williams, D. L.; Heller, A. *J. Phys. Chem.* **1970**, *74*, 4473.
(23) Sinha, H. K.; Dogra, S. K. *Chem. Phys.* **1986**, *102*, 337.
(24) Das, K.; Sarkar, N.; Majumdar, D.; Bhattacharyya, K. *Chem. Phys. Lett.* **1992**, *198*, 443.
(25) Das, K.; Sarkar, N.; Ghosh, A. K.; Majumdar, D.; Nath, D. N.; Bhattacharyya, K. *J. Phys. Chem.* **1994**, *98*, 9126.
(26) Douhal, A.; Amat-Guerri, F.; Lillo, M. P.; Acuña, A. U. *J. Photochem. Photobiol., A* **1994**, *78*, 127.
(27) Mosquera, M.; Penedo, J. C.; Ríos Rodríguez, M. C.; Rodríguez-Prieto, F. *J. Phys. Chem.* **1996**, *100*, 5398.
(28) Ríos, M. A.; Ríos, M. C. *J. Phys. Chem. A* **1998**, *102*, 1560.
(29) Ríos Vázquez, S.; Ríos Rodríguez, M. C.; Mosquera, M.; Rodríguez-Prieto, F. *J. Phys. Chem. A* **2008**, *112*, 376.
(30) Rodríguez Prieto, F.; Ríos Rodríguez, M. C.; Mosquera González, M.; Ríos Fernández, M. A. *J. Phys. Chem.* **1994**, *98*, 8666.
(31) Mosquera, M.; Ríos Rodríguez, M. C.; Rodríguez-Prieto, F. *J. Phys. Chem. A* **1997**, *101*, 2766.
(32) Penedo, J. C.; Mosquera, M.; Rodríguez-Prieto, F. *J. Phys. Chem. A* **2000**, *104*, 7429.
(33) Douhal, A.; Amat-Guerri, F.; Acuña, A. U.; Yoshihara, K. *Chem. Phys. Lett.* **1994**, *217*, 619.
(34) Hein, D. W.; Alheim, R. J.; Leavitt, J. J. *J. Am. Chem. Soc.* **1957**, *79*, 427.
(35) Melhuish, W. H. *J. Phys. Chem.* **1961**, *65*, 229.
(36) Crosby, G. A.; Demas, J. N. *J. Phys. Chem.* **1971**, *75*, 991.
(37) Frisch, M. J.; Trucks, G. W.; Schlegel, H. B.; Scuseria, G. E.; Robb, M. A.; Cheeseman, J. R.; Montgomery J. A., Jr.; Vreven, T.; Kudin, K. N.; Burant, J. C.; Millam, J. M.; Iyengar, S. S.; Tomasi, J.; Barone, V.; Mennucci, B.; Cossi, M.; Scalmani, G.; Rega, N.; Petersson, G. A.; Nakatsuji, H.; Hada, M.; Ehara, M.; Toyota, K.; Fukuda, R.; Hasegawa, J.; Ishida, M.; Nakajima, T.; Honda, Y.; Kitao, O.; Nakai, H.; Klene, M.; Li, X.; Knox, J. E.; Hratchian, H. P.; Cross, J. B.; Bakken, V.; Adamo, C.; Jaramillo, J.; Gomperts, R.; Stratmann, R. E.; Yazyev, O.; Austin, A. J.; Cammi, R.; Pomelli, C.; Ochterski, J. W.; Ayala, P. Y.; Morokuma, K.; Voth, G. A.; Salvador, P.; Dannenberg, J. J.; Zakrzewski, V. G.; Dapprich, S.; Daniels, A. D.; Strain, M. C.; Farkas, O.; Malick, D. K.; Rabuck, A. D.; Raghavachari, K.; Foresman, J. B.; Ortiz, J. V.; Cui, Q.; Baboul, A. G.; Clifford, S.; Cioslowski, J.; Stefanov, B. B.; Liu, G.; Liashenko, A.; Piskorz, P.; Komaromi, I.; Martin, R. L.; Fox, D. J.; Keith, T.; Al-Laham, M. A.; Peng, C. Y.; Nanayakkara, A.; Challacombe, M.; Gill, P. M. W.; Johnson, B.; Chen, W.; Wong, M. W.; Gonzalez, C.; Pople, J. A. *Gaussian '03*; Gaussian, Inc.: Wallingford CT, 2004.
(38) Jolliffe, I. T. *Principal Component Analysis*; Springer-Verlag: New York, 1986.
(39) Al-Soufi, W.; Novo, M.; Mosquera, M. *Appl. Spectrosc.* **2001**, *55*, 630.
(40) Katritzky, A. R. *Handbook of Heterocyclic Chemistry*; Pergamon Press: New York, 1985.
(41) Lee, J.; Robinson, G. W.; Webb, S. P.; Philips, L. A.; Clark, J. H. *J. Am. Chem. Soc.* **1986**, *108*, 6538.
(42) Penedo, J. C.; Ríos Rodríguez, M. C.; García Lema, I.; Pérez Lustres, J. L.; Mosquera, M.; Rodríguez-Prieto, F. *J. Phys. Chem. A* **2005**, *109*, 10189.
(43) Bräuer, M.; Mosquera, M.; Pérez-Lustres, J. L.; Rodríguez-Prieto, F. *J. Phys. Chem. A* **1998**, *102*, 10736.
(44) Ríos Rodríguez, M. C.; Rodríguez-Prieto, F.; Mosquera, M. *Phys. Chem. Chem. Phys.* **1999**, *1*, 253.

JP8076003